Macromolecules

Article

pubs.acs.org/Macromolecules

Using Janus Nanoparticles To Trap Polymer Blend Morphologies during Solvent-Evaporation-Induced Demixing

Kyle C. Bryson,[†] Tina I. Löbling,[‡] Axel H. E. Müller,*[,‡,§] Thomas P. Russell,*[,†] and Ryan C. Hayward*[,†]

[†]Department of Polymer Science and Engineering, University of Massachusetts Amherst, Amherst, Massachusetts 01003, United States

[‡]Makromolekulare Chemie II and Bayreuther Zentrum für Kolloide und Grenzflächen, Universität Bayreuth, 95440 Bayreuth, Germany

[§]Institute of Organic Chemistry, Johannes Gutenberg University Mainz, Duesbergweg 10-14, D-55128 Mainz, Germany

Supporting Information

ABSTRACT: Using ternary blends of polystyrene (PS), poly(methyl methacrylate) (PMMA), and Janus particles (JPs) with symmetric PS and PMMA hemispheres, we demonstrate the stabilization of dispersed and bicontinuous phase-separated morphologies by the interfacial adsorption of Janus particles during demixing upon solvent removal. The resulting blend morphology could be varied by changing the blend composition and JP loading. Increasing particle loading decreased the size of phase-separated domains, while altering the mixing ratio of the PS/PMMA homopolymers produced morphologies ranging from PMMA droplets in a PS matrix to PS droplets in a PMMA matrix. Notably, bicontinuous morphologies were obtained at intermediate blend compositions, marking the first report of highly continuous domains obtained through demixing in a polymer blend compatibilized by Janus particles. The JPs were found to assemble in a densely packed monolayer at the interface, allowing for the stabilization of bicontinuous morphologies in films above the glass transition temperature by inhibiting coarsening and coalescence of the phase-separated domains. The rate of solvent evaporation from the drop-cast films and the molecular weights of the homopolymers were found to greatly affect blend morphology.

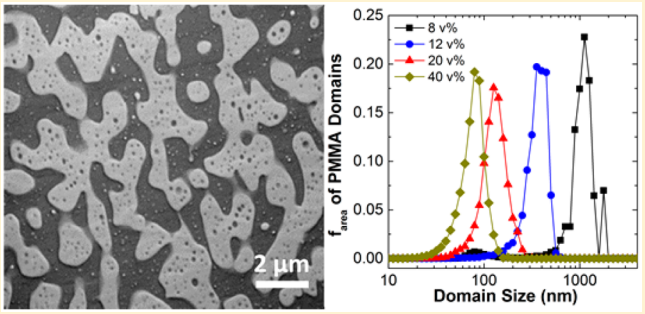

INTRODUCTION

Blending immiscible polymers to produce materials that combine properties of the individual components is an appealing strategy to generate high-performance materials. If the polymer blends can be produced with bicontinuous morphologies, systems with useful transport properties[1,2] are enabled, and routes to mechanically reinforced soft, functional materials become possible.[3] Because of the inherent immiscibility of most polymer pairs, however, surface-active agents are often necessary to prevent macroscopic phase separation. These surfactants decrease interfacial tension and inhibit coalescence of domains by suppressing capillary bridge formation and providing steric stabilization,[4−6] thereby allowing control over the size scale and structure of the phase-separated morphology.

Surfactants such as block copolymers (BCPs) and colloidal particles with homogeneous surface chemistry have received extensive attention as compatibilizers in polymer blends. Block copolymer compatibilizers are effective at hindering coarsening in blends with both dispersed and bicontinuous morphologies[7−10] and have also been used to create thermodynamically stable bicontinuous polymeric microemulsions.[11,12] The overall performance of a BCP compatibilizer involves striking a balance between its diffusion rate (i.e., its ability to reach the interface over the relevant time scale for coalescence of domains), tendency to form micelles, and ability to provide effective steric stabilization. Reactive compatibilization, wherein block copolymers are formed *in situ* at the interface via reaction of end groups, solves the problem of BCP micellization but adds complexity with respect to synthesis and processing.[13,14]

Colloidal particles with homogeneous surface chemistry have also been used as compatibilizers for producing bicontinuous structures in polymer blend systems.[15,16] Composto and coworkers employed interfacially active silica nanoparticles with grafted PMMA to induce kinetic arrest of bicontinuous structures during spinodal decomposition of a PMMA/SAN blend.[17,18] Li et al. demonstrated similar results in a system where the particles were poorly dispersed and not interfacially active, leading to a gel of CdSe−TOPO nanoparticles within the PVME domain of a PS/PVME blend undergoing spinodal decomposition, kinetically arresting the bicontinuous structure.[19] These reports extended the concept of "bijels"[20−22] (bicontinuous, kinetically stabilized emulsion gels), formed by the jamming of neutrally wetting particles at the interface of

Received: March 26, 2015
Revised: May 6, 2015
Published: June 14, 2015

DOI: 10.1021/acs.macromol.5b00640
Macromolecules 2015, 48, 4220−4227

low molecular weight fluids during demixing, to polymeric systems.

Homogeneous colloidal surfactants, while boasting high adsorption energies that render them practically immovable from the interface, face complications in their use to stabilize polymer blends. Particles will adsorb to an A−B interface only if the difference between the interfacial tension values for the particles with each component is less than the A−B interfacial tension, as shown in eq 1,[23] where γ_{AB} represents interfacial tension of A and B phases, and γ_{PA} and γ_{PB} are the interfacial tensions between the particle and A and B phases, respectively:

$$|\gamma_{PA} - \gamma_{PB}| < \gamma_{AB} \quad (1)$$

The low interfacial tension between most immiscible polymer pairs often leads to preferential wetting of the particle by one component. Interfacial adsorption will not occur if the preference is strong, and the particles instead will localize in one phase of the blend.[6] Generating particles without a strong preference for either phase in a mixture with low interfacial tension requires precise control over surface-modifying chemical reactions, which can be difficult to achieve.

Using Janus particles with grafted polymer chains as surfactants in polymer mixtures mitigates the difficulty of achieving interfacial adsorption encountered when using particles with a single type of surface chemistry. Janus particles afford the opportunity to match the chemistries of the polymer chains attached to the particles to those of blend components as well as to control the relative areas of the two different types of polymers on the particle surface (the "Janus balance"). Binks and Fletcher showed that these two variables, i.e., the wettability of each region on the JP with each matrix component and the Janus balance, determine the adsorption energy and contact angle of a JP at an interface.[24] When chemistries are matched, terms γ_{PA} and γ_{PB} in eq 1 become very close to zero, meaning that interfacial adsorption is favored, even if the original surface tension, γ_{AB}, is small, as in polymer blends. Furthermore, in cases where γ_{PA} and γ_{PB} are nearly zero, creating symmetric JPs with equal Janus balance ensures that a 90° contact angle on the interface is favored, achieving neutral wetting that does not impart preferential curvature to the domains.[21] Simulations studying the action of JPs on immiscible blends have found that they impede domain-growth kinetics and decrease domain size more than homogeneous particles[25,26] and that they decrease interfacial tension more and require greater energy for desorption than diblock copolymers.[27]

Despite these advantages, comparatively little experimental work[28,29] has been performed using JPs to compatibilize polymer blends, most likely due to the more complicated syntheses required. While many routes to prepare JPs have been reported,[30−34] most approaches yield JPs that are difficult to functionalize with high molecular weight polymer ligands required for entropically favored mixing with matrix chains. Even when the graft and matrix chains are chemically identical, autophobic dewetting of graft and matrix occurs if the matrix polymer size is appreciably larger than that of the grafts, leading to particle aggregation.[35,36] Two notable reports[28,29] overcome this potential problem by producing JPs from polystyrene-*b*-polybutadiene-*b*-poly(methyl methacrylate) (SBM) triblock copolymers, where the high molecular weight polystyrene and poly(methyl methacrylate) outer blocks function as corona chains attached to a cross-linked polybutadiene core. These SBM JPs exhibited a stronger compatibilization effect in melt-mixed PS/PMMA and poly(phenylene ether)/poly(styrene-*co*-acrylonitrile) (PPE/SAN) blends than the SBM triblock copolymer from which they were formed, clearly demonstrating the effectiveness of JPs with high molecular weight corona chains as surfactants in polymeric mixtures, a result previously found in small-molecule mixtures.[37,38] However, the homopolymer ratios investigated were asymmetric, resulting mostly in spherical domains of one component, with percolated network structures formed only under specific shearing conditions. In the current study, we demonstrate that by varying the loading of SBM JPs in conjunction with the homopolymer mixing ratio, we can kinetically trap both bicontinuous and dispersed morphologies with tunable domain sizes in drop-cast films beginning as a single phase via solvent-induced demixing. The dense packing of the particles at the interface obtained during demixing imparts excellent stability against coalescence and coarsening of domains, preserving the bicontinuous structure when blends are quiescently annealed above the glass transition temperatures of the components for several days.

EXPERIMENTAL SECTION

Polystyrene (M_n = 47 400 g mol^{-1}, PDI = 1.10) was purchased from Polymer Source. Poly(methyl methacrylate) (M_n = 61 800 g mol^{-1}, PDI = 1.51) was synthesized by conventional free radical polymerization. Tetrahydrofuran (THF, Fisher), isopropanol (Fisher), and 1,4-dioxane (Sigma-Aldrich) were used as received. Polystyrene−polybutadiene−poly(methyl methacrylate) Janus particles (SBM JPs), the structure of which is shown schematically in Figure 1a,

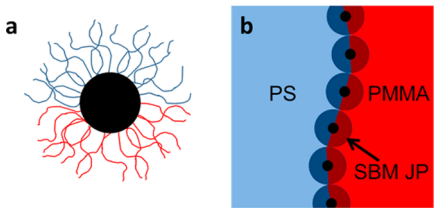

Figure 1. (a) Schematic representation of the structure of the SBM JPs, with cross-linked PB cores (black) and PS (blue) and PMMA (red) grafted chains. (b) Schematic representation of the assembly of the SBM JPs at the PS/PMMA interface.

were prepared from polystyrene-*b*-polybutadiene-*b*-poly(methyl methacrylate) triblock copolymers with respective block molecular weights of 43, 22, and 43 kg/mol. A detailed account of the synthesis of these particles has been published elsewhere.[29,39,40] Briefly, selective precipitation of the middle polybutadiene block produces discrete micellar particles composed of several copolymer chains; these micelles have a PB core and a mixed PS/PMMA grafted chains. Then, the PS chains in the graft layer are selectively precipitated and the PB cores are cross-linked, forming a multicompartment micelle, which, upon the addition of a good solvent for both PS and PMMA, yields dispersed Janus particles. The total density of grafts on the surface is ∼0.08 nm^{-2}. Matrix homopolymer molecular weights were chosen to be similar to the graft molecular weights to ensure entropically favored mixing of graft and matrix chains, allowing for particle assembly at the PS/PMMA interface (depicted schematically in Figure 1b).

The amount of free homopolymer impurity in the Janus particles (e.g., resulting from premature termination during growth of the triblock copolymer precursor) was quantified by soaking a known mass of JP powder in acetic acid and, in a separate vial, cyclohexane, to extract PMMA and PS homopolymers, respectively. To determine the mass of the extracted homopolymer, we used NMR spectroscopy (Bruker DPX300), comparing the signal intensity of peaks corresponding to each polymer to those of a solvent standard of

DOI: 10.1021/acs.macromol.5b00640
Macromolecules 2015, 48, 4220−4227

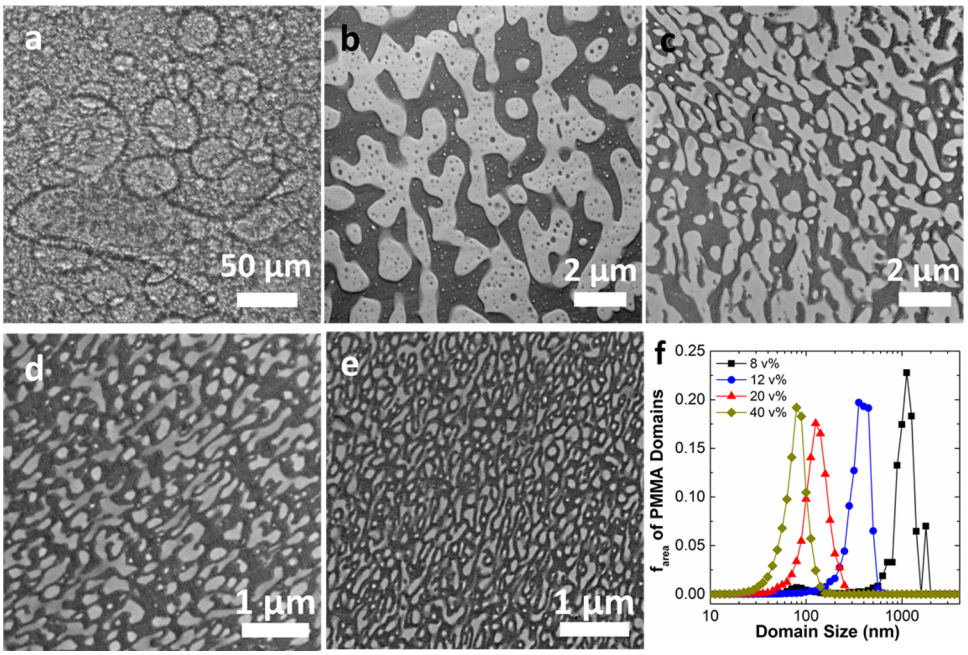

Figure 2. (a–e) Images demonstrating the change in domain size with varying loadings of SBM JPs in 44:56 PS:PMMA (as cast). (a) Optical image of blend with 0 vol % SBM JP, and TEM micrographs of blends with (b) 8, (c) 12, (d) 20, and (e) 40 vol % SBM JP loadings. The dark gray phase in the micrographs is PS; the light gray phase is PMMA. (f) Histogram plot of the area-weighted fraction of PMMA domains as a function of domain size (chord length), as determined by image analysis.

known concentration. The SBM JPs contained less than 5 wt % homopolymer chains. Similarly, selective extraction of PMMA homopolymer from blend films was accomplished by soaking in acetic acid for 1 h.

Solutions of the three blend components were prepared by combining stock solutions of each material to yield 9 wt % total polymer concentration in THF, which is a slightly preferential solvent for PS,[41,42] or 3:1 1,4-dioxane:isopropanol, which is preferential for PMMA. Blend films were cast by dropping 70 μL of the solution onto a glass coverslip; demixing and vitrification occurred during the evaporation process. The films were dried in air for at least 45 min and then under vacuum at 70 °C overnight. Some samples were annealed in a vacuum oven at 160 °C for 4 days. The final film thickness was 30–50 μm.

For imaging, the films were embedded in epoxy and sectioned using a Reichert-Jung Ultracut E microtome and characterized using a JEOL 2000FX transmission electron microscope. To visualize the SBM JPs within the film, the residual PB double bonds were stained with OsO_4 vapor for 90 min; achieving contrast between PS and PMMA did not require staining. Scanning electron micrographs were acquired using a JEOL JCM-5000. Optical micrographs were collected using an Olympus BX51 microscope. Digital image analysis was implemented for quantitative analysis of domain size and shape. Background shading gradients were corrected using an ImageJ plug-in[43] that divided the image by a least-squares polynomial fit of its brightness profile. Using Matlab, the images then were converted to binary, and the area, A, perimeter, p, domain size (chord length, defined as $\pi A/p$), and circularity (defined as $4\pi A/p^2$) of each domain were computed. Histograms of PMMA domain size and circularity distributions were weighted by area by dividing the sum of the areas of the domains contained within each bin by the sum of all domain areas.

RESULTS AND DISCUSSION

Motivated by previous studies showing the effectiveness of JPs for stabilization of blends in melt-mixed systems,[28,29] here we investigate the behavior across a range of compositions in a PS/PMMA/SBM JP ternary blend using solvent-induced phase separation. We first consider the behavior of nearly symmetric blends of PS and PMMA cast from THF, an almost nonselective solvent for PS and PMMA. In samples without SBM JPs, optical micrographs such as in Figure 2a reveal the formation of very large domains (sizes up to ~100 μm), as expected for a blend lacking any compatibilizers. Transmission electron micrographs in Figures 2b–e show the as-cast structure of the PS/PMMA/SBM JP ternary blend as the particle loading increases from 8 to 40 vol %. This increase gives rise to a decrease in average domain size from about 1000 to about 75 nm. Importantly, the morphology obtained at 8 vol % is bicontinuous, as confirmed by the fact that PMMA domains can be selectively extracted by soaking the film in acetic acid for 1 h, as shown in Supporting Information Figure 1. Samples with 60 vol % loading show a further decrease in domain size and a transition to a lamellar morphology (Supporting Information Figure 2a), a finding predicted in simulation for JPs in a binary mixture.[44] Greater concentrations of particles cause the coalescence process to be halted earlier during phase separation, stabilizing smaller scale structures, similar in size to those formed during melt-mixing experiments with JPs as compatibilizers.[28]

Further analysis of the size of the PMMA domains confirms and quantifies visual observations of morphological change brought about by the interfacial adsorption of SBM JPs. A histogram of the PMMA domain size distribution, weighted by the fraction of total domain area contained within each bin, is shown in Figure 2f. The data comprise at least six micrographs per sample. Unfortunately, a characteristic domain size could not be obtained from Fourier analysis of images at low JP loadings. Thus, we instead quantify domain size in terms of the chord length using an expression applicable to domains of arbitrary shape; these values closely match those obtained by manual measurement. In the 8 vol % SBM JP sample, a significant population of small domains and micelles exists, possibly because the low particle loading leads to more

DOI: 10.1021/acs.macromol.5b00640
Macromolecules 2015, 48, 4220–4227

prevalent coarsening during the early stages of phase separation, yielding large interdomain separations that decrease diffusion of the particles to an interface. Additionally, at low particle loadings, we observe small, particle-stabilized domains of PS in the PMMA phase at some blend compositions, evidence of secondary phase separation that likely occurs due to the faster rate of coarsening compared to diffusion through the large domains. The length scale of the phase-separated structures becomes more homogeneous and monomodal as particle loading increases.

In a phase-separated system bearing a close-packed particle monolayer adsorbed at the interface, the characteristic domain size, ξ, here taken to be the peak domain size, varies inversely with particle volume fraction as given in eq 2[21,22,45−47]

$$\xi \propto \frac{d}{\phi} \tag{2}$$

where d is particle diameter and ϕ is particle volume fraction. For samples with 12−40 vol % SBM JP, the characteristic domain size is in reasonable agreement with this dependence (Supporting Information Figure 3), suggesting that the particles adopt a close-packed arrangement at the interface. Electron microscopy confirms this finding, showing that the particles, marked by dark OsO_4-stained PB cores, form a densely packed, interfacially adsorbed layer between PS and PMMA domains (Figure 3). No evidence of free SBM JPs dispersed in either phase was observed for these molecular weights and processing conditions. The PS/PMMA interface is always observed to be saturated with densely packed SBM JPs, whose center-to-center distance at the interface is ≈20 nm. The smallest gaps between the edges of polybutadiene cores is ≈10 nm (Figure 3), comparable to twice the ideal end-to-end distance of the corona chains, about ≈ 6 nm for 43 kg/mol polystyrene,[48] indicating minimal overlap or interpenetration of the adsorbed SBM JPs at the interface. Interestingly, the best-fit line relating ξ to ϕ^{-1} at high particle loadings (Supporting Information Figure 3) has a slope of 36 nm, which closely matches the sizes expected for spherical domains stabilized by a close-packed monolayer of spherical particles with d = 20 nm, i.e., $\pi d/\sqrt{3} \approx 36$ nm. A similar result was also obtained by Herzig et al.[21] for bicontinuous structures on a size scale of tens of microns bearing a high-density monolayer of particles. In the current system, the characteristic size scale for films with 8 vol % SBM JP falls well above the linear fit obtained for the samples with 12−40 vol %, likely due to the large number of small domains seen at 8 vol %, which leads to an effectively lower particle loading for the larger domains that dominate the area-weighted histogram of domain sizes.

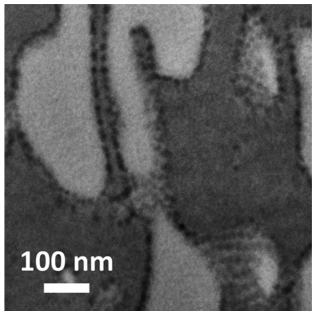

Figure 3. TEM micrograph illustrating the densely packed structure of the SBM JPs at the PS:PMMA interface in a 44:56 PS:PMMA + 20 vol % SBM JP blend. The center-to-center distance is about 20 nm, while the particle cores are separated by 10 nm, approximately twice the size of the grafted chains.

Varying the ratio of PS/PMMA homopolymers in the presence of SBM JPs has a dramatic effect on the resulting morphology. For PS:PMMA compositions from 54:46 to 33:67 PS:PMMA with 8 vol % SBM JPs, the morphology undergoes a transition from PMMA droplets in a PS matrix to PS droplets in a PMMA matrix and in-between passing through a range of compositions where the domains of both materials are elongated and show some degree of percolation (Figures 4a−e), with 44:56 PS:PMMA displaying a bicontinuous morphology (Supporting Information Figure 1).

At higher loading of JPs, the evolution of blend morphology with PS/PMMA ratio is slightly different, as shown in Figure 5 for 20 vol % SBM JP loading. Comparing Figures 4 and 5, it is clear that at equivalent PS:PMMA ratios the greater loading of JPs leads to an increase in the dispersion of PMMA domains and, correspondingly, in the continuity of PS domains. The PS:PMMA ratio at which the sample appears to have the greatest degree of bicontinuity shifts from 44:56 at 8 vol % SBM JP to 40:60 PS:PMMA at 20 vol %. Additionally, while phase inversion from PMMA-in-PS to PS-in-PMMA is seen at about 40:60 PS:PMMA with 8 vol % SBM JP, samples with 20 vol % SBM JP still exhibit highly continuous PS domains even at 25:75 PS:PMMA, although the PMMA domains are also highly interconnected (Supporting Information Figure 2b). These loading-dependent morphology changes, combined with observations that JPs disperse (as micelles) exclusively in the PS domains, not in PMMA domains, at all but the lowest particles loadings investigated, point to the SBM JPs possessing a slight preference for PS. The genesis of this preference may be the polybutadiene cores of the particles, which interact more favorably with PS than PMMA.[49] Since the grafting density of the SBM JPs is low, the cores may interact with the matrix homopolymers, increasing the wettability of particles by PS. However, because this blend system is capable of forming bicontinuous structures and undergoing phase inversion, the preference for PS must be fairly weak.[50] The relatively high loading of particles used here also raises the possibility that preferential partitioning of JPs into the PS phase could increase the viscosity relative to that of PMMA, possibly helping to enforce continuity in the PS phase by a viscoelastic phase separation mechanism.[51] However, as the majority of JPs are found to be interfacially adsorbed, rather than dispersed within the PS phase, we expect that interfacial stabilization effects dominate over those of dynamic asymmetry.

We explored whether the slight preference of THF as a solvent for PS over PMMA might play a role in the development of JP-stabilized blend morphology. The poorer solvation and higher molecular weight of the PMMA homopolymer could lead to its precipitation before PS, bringing about a preference for a dispersed PMMA morphology. To investigate this hypothesis, we studied blends cast from a solvent preferential to PMMA. Employing a 33:67 PS:PMMA blend composition, where PS droplets were observed with 8 vol % SBM JP loading but not with 20 vol % loading, we used a 3:1 (v:v) 1,4-dioxane:isopropanol solvent mixture, whose isopropanol content is nearly the maximum concentration that still will dissolve PS, and cast films at 48 °C, at which the solvent mixture has a vapor pressure approximately equal to that of THF at room temperature. The morphology of the resulting film containing 20 vol % JPs, shown in Supporting Information

DOI: 10.1021/acs.macromol.5b00640
Macromolecules 2015, 48, 4220−4227

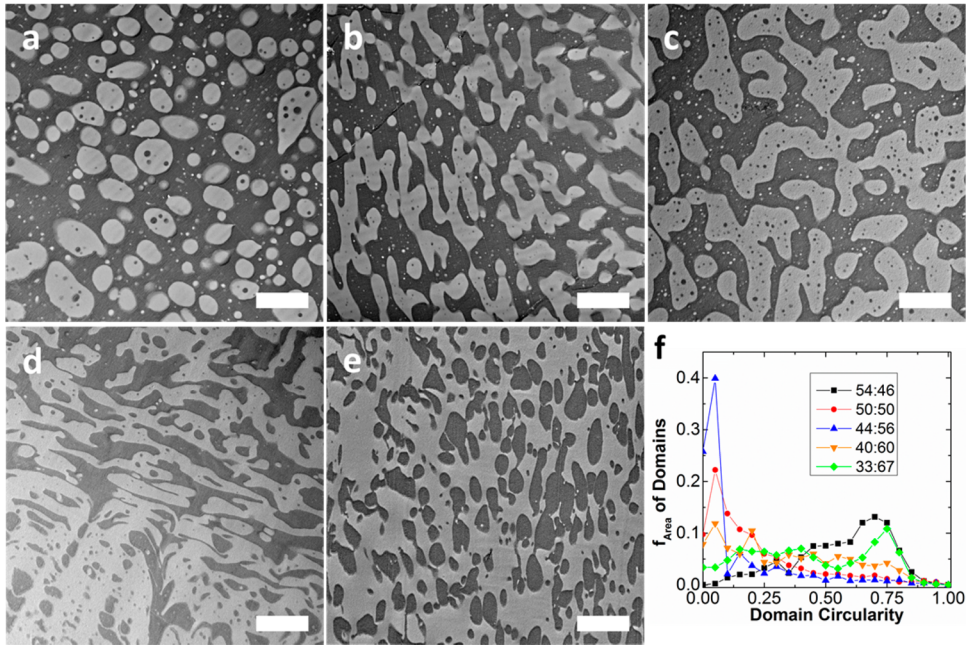

Figure 4. TEM micrographs demonstrating the change in domain shape of PS/PMMA blends with 8 vol % SBM JPs in response to changes in blend composition: (a) 54:46, (b) 50:50, (c) 44:56, (d) 40:60, and (e) 33:67 PS:PMMA. Scale bars represent 2 μm. (f) Histogram plot of the area-weighted fraction of dispersed domains as a function of their circularity, as determined by image analysis.

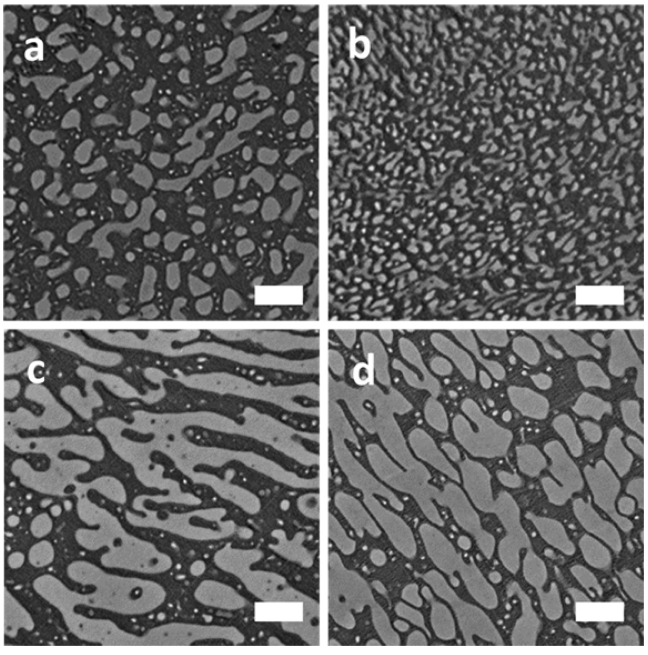

Figure 5. TEM micrographs demonstrating change in domain shape of PS/PMMA blends with 20 vol % SBM JPs in response to changes in blend composition: (a) 47:53, (b) 44:56, (c) 40:60, (d) 33:67 PS:PMMA. Scale bars represent 1 μm.

Figure 4, closely resembles that of the film cast from THF. Given this near insensitivity of morphology to a change in solvent preference, we attribute the loading-dependent morphology changes seen here primarily to a slight PS-preference of the SBM JPs.

We demonstrate that interfacially adsorbed SBM JPs confer structural stability to this blend system, similar to that observed in bijels of small-molecule liquids. Previously, the excellent stability of SBM JP-stabilized blends was ascribed by Müller and co-workers to arise from the same close packing and interfacial saturation that we observe in our blends.[28] In a poorly compatibilized system, coalescence during annealing causes an increase in domain size and circularity to increase the volume/surface area ratio. This is evident in pure PS/PMMA blends with no added particles, where annealing at 160 °C for 4 days (Figure 6a, as-cast structure shown in Figure 2a) brings about an extreme change in morphology. While holding the sample at this temperature, 50−60 °C above T_g, the already large domains coalesce such that the film possess a bilayer structure consisting of one PS and one PMMA domain, with some small dispersed secondary domains (cross-sectional image in Figure 6a inset). In samples containing JPs, we see much less change in morphology. Figure 6b shows the morphology of the 44:56 PS:PMMA sample with 8 vol % SBM JP, whose as-cast structure is shown in Figure 2b, after annealing at 160 °C for 4 days. Plots comparing the sizes and circularity of the domains before and after annealing (Figure 6d) show a small decrease in domain size and increase in circularity, likely a result of a slight loss of bicontinuity upon annealing. In films with 20 vol % JPs (Figure 6c, as-cast structure shown in Figure 2d), modest increases in domain size and circularity are observed (Figure 6e). For both samples, the increased circularity reflects a shift in the dispersed PMMA domains toward more spherical structures without extensive coalescence. Presumably, the greater Laplace pressure experienced by the smaller domains is more easily able to drive desorption or rearrangement of JPs in the samples with higher loading, explaining the greater morphological changes observed. The fact that domains can undergo some degree of morphological change upon annealing suggests that particles may not truly be irreversibly jammed at the interface. Nevertheless, observations of close-packed, adjacent particle monolayers (Figure 3) together with very limited coarsening indicate that SBM JPs provide highly stable, bicontinuous morphologies quite similar to bijel structures obtained through particle jamming.

DOI: 10.1021/acs.macromol.5b00640
Macromolecules 2015, 48, 4220−4227

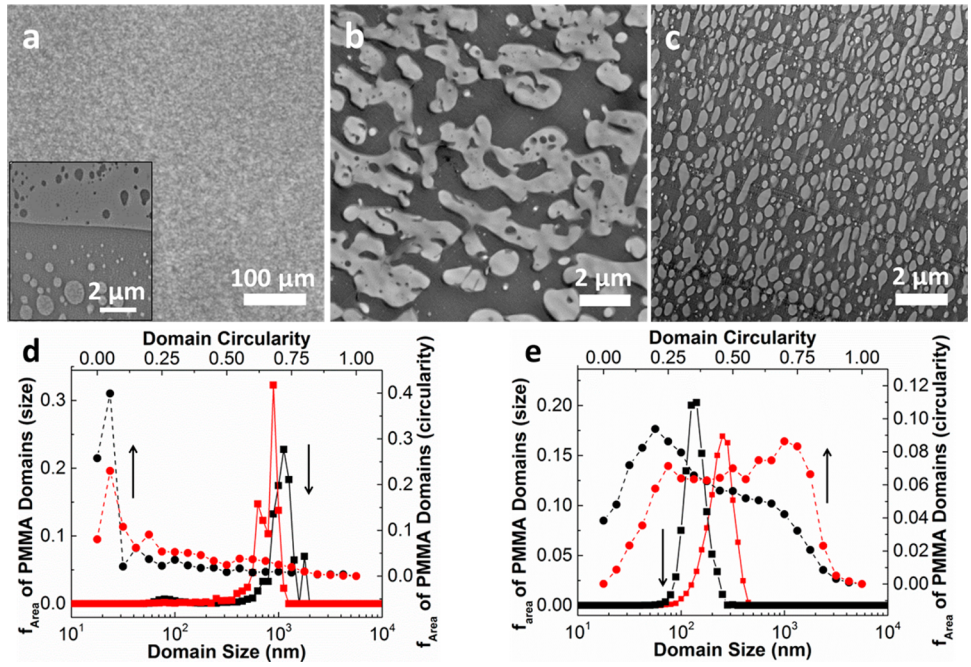

Figure 6. Images of morphology after annealing of 44:56 PS:PMMA samples for 4 days at 160 °C, for comparison to as-cast structures shown in Figures 2a,b,d. (a) Optical micrograph of 0% JP blend (inset: TEM micrograph of film cross section) and TEM micrographs of (b) 8 and (c) 20 vol % JP. Area-weighted distributions of PMMA domain size (solid lines) and circularity (dotted lines) for both as-cast (black) and annealed (red) for (d) 8 and (e) 20 vol % SBM JP.

We note that the solvent evaporation rate can play an important role in determining the morphology of the materials studied here. During drying of a solution, the polymer concentration near the solution−air interface increases more rapidly than that near the substrate, creating a viscous barrier ("skin layer") that inhibits subsequent solvent evaporation from deeper within the film. Thus, solvent concentration decreases more slowly closer to the substrate, increasing the time between the onset of phase separation and vitrification[52] and leading to secondary phase separation, coarsening, and relaxation of elongated shapes in solvent-swollen domains. In samples cast at room temperature, greater circularity is routinely observed among domains nearer the substrate−polymer interface than those near the air−polymer interface (Supporting Information Figure 5a); this heterogeneity decreases as loading increases. Increasing the substrate casting temperature intensifies the effect of the skin layer, creating a greater degree of through thickness morphological heterogeneity, likely because more rapid initial solvent evaporation yields a more viscous skin layer that strongly inhibits solvent passage to the air interface. Interestingly, casting at higher temperatures had little effect on domain size in the skin layer but produced larger, more circular structures deep in the film (Supporting Information Figure 5b). Slowly evaporating solvent over the course of several hours decreased the amount of heterogeneity but greatly increased domain size and circularity (Supporting Information Figure 5c). These results indicate that the SBM JPs are not highly effective compatibilizers when demixing begins at high solvent concentrations, likely due to low surface coverage and the very small interfacial tension leading to a preference for dispersion in solution as opposed to adsorption.

We have also performed experiments using matrix homopolymers of lower and higher molecular weights than those discussed above. Higher molecular weight homopolymers (M_n = 127 and 120 kg mol^{-1} for PS and PMMA, respectively) in a 50:50 blend with 8 vol % SBM JP produced large, spherical domains, a sign of poor stabilization by the particles, while films with 20 vol % JP displayed a structure of wormlike PS domains within a PMMA matrix. In this case, SBM JPs were located primarily within the PS phase (Figure 7a), providing further

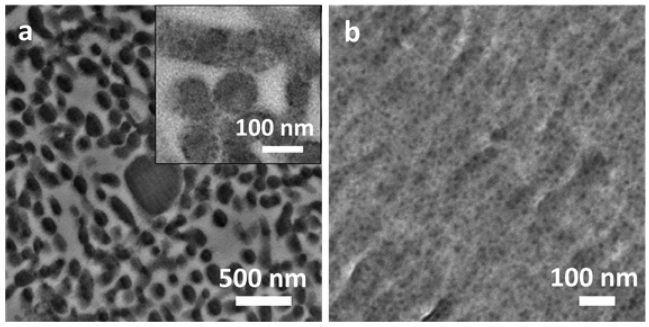

Figure 7. Films with higher and lower molecular weight matrix homopolymers. (a) TEM micrographs of 50:50 PS (127 kg/mol):PMMA (120 kg/mol) + 20 vol % SBM JP (inset: detail showing JP assembly inside PS domains, indicative of preferential interaction of the particles with PS). (b) TEM micrograph showing a phase-mixed structure in 50:50 PS (3.2 kg/mol):PMMA (5.0 kg/mol) + 20 vol % SBM JP, featuring increased core-to-core distance of about 40 nm.

evidence for the preference of the SBM JPs for PS. Annealing this sample at 140 °C for 24 h led to dramatic changes in the as-cast morphology, causing coarsening of the morphology and aggregation of JPs into micelles. These results can be explained by autophobic dewetting and corresponding loss of JP surfactancy due to the inability of the homopolymer chains to wet the much smaller SBM JP grafted chains. When using a 50:50 ratio of lower molecular weight homopolymers (M_n = 3.2 and 5.0 kg mol^{-1} for PS and PMMA, respectively) with 8 vol % SBM JP, films possess small, spherical PMMA domains about

DOI: 10.1021/acs.macromol.5b00640
Macromolecules 2015, 48, 4220−4227

100 nm in diameter dispersed in PS, while with 20 vol % SBM JP loading samples are optically clear and appear to be single-phase, with particles uniformly dispersed with greater core-to-core distances than when assembled at the interface (Figure 7b). Similar observations of additives altering phase behavior have been observed in ternary blends of homopolymers and block copolymers[53,54] and concentrated colloidal suspensions in small molecule liquids.[55] On the basis of the range of χ values reported in the literature for PS−PMMA at room temperature (approximately 0.03−0.06),[56] and the average degree of polymerization of the polymers (N = 40), we estimate χN to be 1.2−2.4. Thus, while the system clearly does phase separate in the absence of JPs, it is apparently very close to the critical value for phase separation of $\chi N \approx 2$, and hence addition of relatively large amounts of JPs is sufficient to form a single-phase mixture.

In conclusion, using a ternary blend of PS, PMMA, and interfacially active Janus particles based on PS-*b*-PB-*b*-PMMA triblock copolymers, we could control blend morphology formed by demixing in solvent-cast films through variations in the volume fraction of particles and the homopolymer composition ratio. Samples possessing percolated domains of both PS and PMMA were obtained, and these structures showed good resistance to coarsening during several days of annealing well above the glass transition temperatures of the components thanks to the saturation of the interfaces with nearly close-packed layers of particles. When higher molecular weight homopolymers were used, phase-separated domains were poorly stabilized and coalesced above the glass transition temperature of the components, while low molecular weight homopolymers brought about miscibility in the three-component system at the same particle loading. On the basis of these results, we suggest that Janus nanoparticles with appropriately chosen graft molecular weights should provide a robust means to stabilize bicontinuous, bijel-like morphologies in polymer blends.

■ ASSOCIATED CONTENT

Supporting Information

Further evidence for bicontinuity, morphologies obtained at other compositions and casting conditions, and the relationship of domain size and particle loading. The Supporting Information is available free of charge on the ACS Publications website at DOI: 10.1021/acs.macromol.5b00640.

■ AUTHOR INFORMATION

Corresponding Authors

*(R.C.H.) E-mail hayward@umass.edu; Tel 413-577-1317; Fax 413-545-0082.

*(T.P.R.) E-mail russell@mail.pse.umass.edu; Tel 413-577-1516; Fax 413-545-0082.

*(A.H.E.M.) E-mail axel.mueller@uni-mainz.de; Tel +49 (6131) 3922372.

Notes

The authors declare no competing financial interest.

■ ACKNOWLEDGMENTS

This work was primarily supported by Polymer-Based Materials for Harvesting Solar Energy, an Energy Frontier Research Center funded by the U.S. Department of Energy, Office of Science, Basic Energy Sciences, under Award DE-SC0001087 (morphological studies), with additional support from Deutsche Forschungsgemeinschaft (Mu896/39; Janus NP preparation). The work also made use of facilities supported by the National Science Foundation MRSEC at UMass (DMR-0820506). K.C.B. acknowledges the National Science Foundation for support through a Graduate Research Fellowship (Grant DGE-0907995).

■ REFERENCES

(1) Hoppe, H.; Sariciftci, N. S. *J. Mater. Chem.* **2006**, *16*, 45−61.
(2) Kreuer, K. D. *J. Membr. Sci.* **2001**, *185*, 29−39.
(3) Walker, C. N.; Bryson, K. C.; Hayward, R. C.; Tew, G. N. *ACS Nano* **2014**, *8*, 12376−12385.
(4) Binks, B. P. *Curr. Opin. Colloid Interface Sci.* **2002**, *7*, 21−41.
(5) Aveyard, R. J.; Binks, B. P.; Clint, J. H. *Adv. Colloid Interface Sci.* **2003**, *100*, 503−546.
(6) Fenouillot, F.; Cassagnau, P.; Majeste, J.-C. *Polymer* **2009**, *50*, 1333−1350.
(7) Lepers, J.-C.; Favis, B. D.; Lacroix, C. *J. Polym. Sci., Part B: Polym. Phys.* **1999**, *37*, 939−951.
(8) Lyu, S.-P.; Jones, T. D.; Bates, F. S.; Macosko, C. W. *Macromolecules* **2002**, *35*, 7845−7855.
(9) Galloway, J. A.; Jeon, H. K.; Bell, J. R.; Macosko, C. W. *Polymer* **2005**, *46*, 183−191.
(10) Bell, J. R.; Chang, K.; Lopez-Barron, C. R.; Macosko, C. W.; Morse, D. C. *Macromolecules* **2010**, *43*, 5024−5032.
(11) Bates, F. S.; Maurer, W. W.; Lipic, P. M.; Hillmyer, M. A.; Almdal, K.; Mortensen, K.; Fredrickson, G. H.; Lodge, T. P. *Phys. Rev. Lett.* **1997**, *79*, 849−852.
(12) Hillmyer, M. A.; Maurer, W. W.; Lodge, T. P.; Bates, F. S.; Almdal, K. *J. Phys. Chem. B* **1999**, *103*, 4814−4824.
(13) Pötschke, P.; Paul, D. R. *J. Macromol. Sci., Polym. Rev.* **2003**, *C43* (1), 87−141.
(14) Sundararaj, U.; Macoscko, C. W. *Macromolecules* **1995**, *28*, 2647−2657.
(15) Gubbels, F.; Blacher, S.; Vanlathem, E.; Jerome, R.; Deltour, R.; Brouers, F.; Teyssie, P. *Macromolecules* **1995**, *28*, 1559−1566.
(16) Clegg, P. S. *J. Phys.: Condens. Matter* **2008**, *20*, 113101.
(17) Chung, H.; Ohno, K.; Fukuda, T.; Composto, R. J. *Nano Lett.* **2005**, *5*, 1878−1882.
(18) Gam, S.; Corlu, A.; Chung, H.-J.; Ohno, K.; Hore, M. J. A.; Composto, R. J. *Soft Matter* **2011**, *7*, 7262−7268.
(19) Li, L.; Miesch, C.; Sudeep, P. K.; Balazs, A. C.; Emrick, T.; Russell, T. P.; Hayward, R. C. *Nano Lett.* **2011**, *11*, 1997−2003.
(20) Stratford, K.; Adhikari, R.; Pagonabarraga, I.; Desplat, J. C.; Cates, M. E. *Science* **2005**, *309* (5744), 2198−2201.
(21) Herzig, E. M.; White, K. A.; Schofield, A. B.; Poon, W. C. K.; Clegg, P. S. *Nat. Mater.* **2007**, *6*, 966−971.
(22) Tavacoli, J. W.; Thijssen, J. H. J.; Schofi eld, A. B.; Clegg, P. S. *Adv. Funct. Mater.* **2011**, *21*, 2020−2027.
(23) Dinsmore, A. D.; Hsu, M. F.; Nikolaides, M. G.; Marquez, M.; Bausch, M. R.; Weitz, D. A. *Science* **2002**, *298*, 1006−1009.
(24) Binks, B. P.; Fletcher, P. D. I. *Langmuir* **2001**, *17*, 4708−4710.
(25) Huang, M.; Li, Z.; Guo, H. *Soft Matter* **2012**, *8*, 6834−6845.
(26) Huang, M.; Guo, H. *Soft Matter* **2013**, *9*, 7356−7368.
(27) Estridge, C. E.; Jayaraman, A. *ACS Macro Lett.* **2015**, *4*, 155−159.
(28) Walther, A.; Matussek, K.; Müller, A. H. E. *ACS Nano* **2008**, *2*, 1167−1178.
(29) Bahrami, R.; Löbling, T. I.; Gröschel, A. H.; Schmalz, H.; Müller, A. H. E.; Altstädt, V. *ACS Nano* **2014**, *8*, 10048−10056.
(30) Walther, A.; Müller, A. H. E. *Chem. Rev.* **2013**, *113* (7), 5194−5261.
(31) Jiang, S.; Chen, Q.; Tripathy, M.; Luijten, E.; Schweizer, K. S.; Granick, S. *Adv. Mater.* **2010**, *22*, 1060−1071.
(32) Du, J.; O'Reilly, R. K. *Chem. Soc. Rev.* **2011**, *40*, 2402−2416.
(33) Wurm, F.; Kilbinger, A. F. M. *Angew. Chem., Int. Ed.* **2009**, *48*, 8412−8421.
(34) Loget, G.; Kuhn, A. *J. Mater. Chem.* **2012**, *22*, 15457−15474.

DOI: 10.1021/acs.macromol.5b00640
Macromolecules 2015, 48, 4220−4227

(35) Sunday, D.; Ilavsky, J.; Green, D. L. *Macromolecules* **2012**, *45*, 4007−4011.
(36) Frischknecht, A. L.; Hore, M. J. A.; Ford, J.; Composto, R. J. *Macromolecules* **2013**, *46*, 2856−2869.
(37) Ruhland, T. M.; Gröschel, A. H.; Walther, A.; Müller, A. H. E. *Langmuir* **2011**, *27*, 9807−9814.
(38) Ruhland, T. M.; Gröschel, A. H.; Ballard, N.; Skelhon, T. S.; Walther, A.; Müller, A. H. E.; Bon, S. A. F. *Langmuir* **2013**, *29*, 1388−1394.
(39) Gröschel, A. H.; Schacher, F. H.; Schmalz, H.; Borisov, O. V.; Zhulina, E. B.; Walther, A.; Müller, A. H. E. *Nat. Commun.* **2012**, *3*, 710.
(40) Gröschel, A. H.; Walther, A.; Löbling, T. I.; Schmelz, J.; Hanisch, A.; Schmalz, H.; Müller, A.H. E. *J. Am. Chem. Soc.* **2012**, *134*, 13850−13860.
(41) Böker, A.; Müller, A.H. E.; Krausch, G. *Macromolecules* **2001**, *34*, 7477−7488.
(42) Peng, J.; Kim, D. H.; Knoll, W.; Xuan, Y.; Li, B.; Han, Y. *J. Chem. Phys.* **2006**, *125*, 064702.
(43) Dougherty, R. "Polynomial Shading Corrector"; http://www.optinav.com/Polynomial_Shading_Corrector.htm (accessed Oct 28, 2014).
(44) Krekhov, A.; Weith, V.; Zimmermann, W. *Phys. Rev. E* **2013**, *88*, 040302(R).
(45) S. Arditty, S.; Whitby, C. P.; Binks, B. P.; Schmitt, V.; Leal-Calderon, F. *Eur. Phys. J. E* **2003**, *11*, 273−281.
(46) Hore, M. J. A.; Laradji, M. *J. Chem. Phys.* **2007**, *126*, 244903.
(47) Witt, J. A.; Mumm, D. R.; Mohraz, A. *Soft Matter* **2013**, *9*, 6773−6780.
(48) Terao, K.; Mays, J. W. *Eur. Polym. J.* **2004**, *40*, 1623−1627.
(49) Stocker, W.; Beckmann, J.; Stadler, R.; Rabe, J. P. *Macromolecules* **1996**, *29*, 7502−7507.
(50) Hunter, T. N.; Pugh, R. J.; Franks, G. V.; Jameson, G. J. *Adv. Colloid Interface Sci.* **2008**, *137*, 57−81.
(51) Tanaka, H. *J. Phys.: Condens. Matter* **2000**, *12*, R207−R264.
(52) Tsige, M.; Grest, G. S. *J. Phys.: Condens. Matter* **2005**, *17*, S4119−S4132.
(53) Riess, G.; Periard, J.; Jolivet, Y. *Angew. Chem., Int. Ed. Engl.* **1972**, *11*, 339.
(54) Dudowicz, J.; Freed, K. F.; Douglas, J. F. *Macromolecules* **1996**, *28*, 2276−2287.
(55) Jayalakshmi, Y.; Kaler, E. W. *Phys. Rev. Lett.* **1997**, *78*, 1379−1382.
(56) Cho, J. *Macromol. Res.* **2011**, *19*, 984−987.

DOI: 10.1021/acs.macromol.5b00640
Macromolecules 2015, 48, 4220−4227